PERGAMON

International Journal of Solids and Structures 40 (2003) 331–342

INTERNATIONAL JOURNAL OF SOLIDS and STRUCTURES

www.elsevier.com/locate/ijsolstr

Three-dimensional Green's functions for composite laminates

F.G. Yuan [a,*], S. Yang [a], B. Yang [b]

[a] *Department of Mechanical and Aerospace Engineering, North Carolina State University, Raleigh, NC 27695, USA*
[b] *Structures Technology Inc., 543 Keisler Drive, Suite 204, Cary, NC 27511, USA*

Received 7 February 2002; received in revised form 19 September 2002

Abstract

The three-dimensional Green's functions due to a point force in composite laminates are solved by using generalized Stroh formalism and two-dimensional Fourier transforms. Each layer of the composite is generally anisotropic and linearly elastic. The interfaces between different layers are parallel to the top and bottom surfaces of the composite and are perfectly bonded. The Green's functions of point forces applied at the free surface, interface, and in the interior of a layer are derived in the Fourier transformed domain respectively. The surfaces are imposed by a proportional spring-type boundary condition. The spring-type condition may be reduced to traction-free, displacement-fixed, and mirror-symmetric conditions. Numerical examples are given to demonstrate the validity and elegance of the present formulation of three-dimensional point-force Green's functions for composite laminates.

Keywords: Anisotropic elasticity; Green's function; Three dimensions; Composite laminates; Stroh formalism; Fourier transforms

1. Introduction

Fundamental three-dimensional Green's functions in the theory of linear elasticity have been studied by many researchers. The Green's function of a point force applied in an infinite isotropic solid was first solved by Kelvin (1848). The Green's functions of a point force perpendicular to and parallel to the plane surface of a semi-infinite isotropic medium have been furnished by Boussinesq (1885) and Cerruti (1888), respectively. A concentrated force, applied at a point in a semi-infinite space, has been considered by Mindlin (1936). Mindlin also showed that the half-space Green's function can be obtained by superposition of 18 nuclei of strain derived from the Kelvin solution.

For three-dimensional generally anisotropic solids, a line integral representation of the Green's function in an infinite medium has been investigated by Fredholm (1900), Lifshitz and Rozenzweig (1947), Synge (1957), and Mura (1987). For the special case of transversely isotropic materials, explicit forms of the Green's function have been obtained by Lifshitz and Rozenzweig (1947), Elliott (1948), Kroner (1953), Willis (1969), Lejcek (1965), and Pan and Chou (1976). Pan and Chou (1979a,b) have developed the Green's

* Corresponding author.
E-mail address: yuan@eos.ncsu.edu (F.G. Yuan).

0020-7683/02/$ - see front matter
PII: S0020-7683(02)00545-0

functions of a point force applied in a semi-infinite and in two semi-infinite transversely isotropic solids. Pan (1997) has derived the static Green's functions in multilayered transversely isotropic and isotropic half-spaces by using the propagator matrix method.

Stroh (1958, 1962) developed a powerful and elegant six-dimensional theory of dislocations, line forces and surface waves in generally anisotropic elastic solids in two dimensions. Unlike the two-dimensional anisotropic solutions developed by Green and Zerna (1954) which are restricted to plane-strain deformation, the Stroh formalism applied to generally anisotropic elastic materials for which all three displacement components are coupled. Also, unlike the Lekhnitskii's formalism (1963) which breaks down for orthotropic materials and requires a special treatment. The method provides solutions for dislocations in terms of eigenvalues and eigenvectors of a six-dimensional eigenvalue problem. Willis (1966) derived the surface Green's function for half-space. Using Stroh formalism, the explicit form of 3-D Green's function of a point force in an infinite generally anisotropic solid has been derived by Barnett and Lothe (1973) in terms of sextic eigenvalue expression. The Green's function of a point force applied at the surface of a semi-infinite generally anisotropic solid has been developed by Barnett and Lothe (1975) using Stroh formalism and Fourier transform technique. They also showed that, by applying two-dimensional Fourier transforms to the 3-D equilibrium equation, the eigenvalues and associated eigenvectors in the transformed space are analogous to the Stroh formalism in two dimensions. Ting (1996) presented the Green's functions for half-space and bimaterials in the two-dimensional Fourier transformed space. Ting and Lee (1997) obtained an explicit expression in terms of Stroh eigenvalues for three-dimensional Green's function in generally anisotropic elastic solids. Wang (1997) provided another explicit expansion for Green's functions in an infinite space by means of integral representation technique and an application of complex variable residual calculus. Recently, Yue (1999) developed a layered Green's function and Pan and Yuan (2000a,b) obtained bimaterial Green's functions including piezoelectric materials.

In this paper, the three-dimensional Green's function due to a point force in multilayered composite laminates is solved by using Stroh formalism and two-dimensional Fourier transforms. Each layer of the material is homogeneous, generally anisotropic, and linearly elastic. The interfaces are parallel to the top and bottom surfaces of the composite and are perfectly bonded. The top and bottom surfaces are imposed by a proportional spring-type boundary condition, which can be reduced to traction-free, displacement-fixed and mirror-symmetric conditions. Since the solutions are first derived in the Fourier transformed domain, Fourier inverse transform has to be carried out to recover the physical quantities. The formulation is described in Section 2. In Section 3, numerical examples are given to demonstrate the validity and elegance of the present formulation of three-dimensional elastostatic Green's functions for generally anisotropic composite laminates. Conclusions are given in Section 4.

2. Formulation

Consider a composite laminate that consists of n layers of different generally anisotropic elastic materials as shown in Fig. 1. Let a Cartesian coordinate system (x_1, x_2, x_3) be chosen such that the x_1–x_2 plane lies on the top surface of the laminate and the composite occupy $x_3 \geqslant 0$. Each layer of the laminate occupies the region $h_{j-1} \leqslant x_3 \leqslant h_j$ $(j = 1, 2, \ldots, n)$ with $0 = h_0 < h_1 < \cdots < h_n$ and the thickness of each layer, δ_k is arbitrary. If $h_n = \infty$, the composite is a layered half-space. Across each interface at $x_3 = h_j$ $(i = 1, 2, \ldots, n-1)$, the continuity condition of displacement and traction is imposed.

The equation of equilibrium in terms of displacement u_k in the absence of body forces is expressed as

$$C_{ijkl} u_{k,lj} = 0, \tag{1}$$

where C_{ijkl} is the elastic stiffness tensor, and the convention of summation on repeated subscript indices over their range is implied. In the following, we derive the general solution of anisotropic materials in Stroh

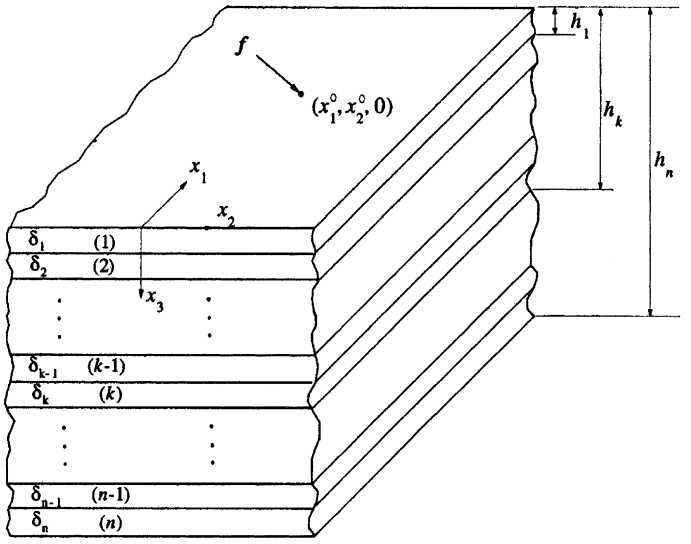

Fig. 1. An n-layered composite laminate.

formalism and Fourier transforms, followed by the Green's function due to a point force for composite laminates.

2.1. General solution in Stroh formalism

By applying two-dimensional Fourier transforms (y_1, y_2) for (x_1, x_2) in Eq. (1), one obtains

$$C_{i\alpha k\beta} y_\alpha y_\beta \tilde{u}_k + \mathrm{i}(C_{i\alpha k3} + C_{i3k\alpha}) y_\alpha \tilde{u}_{k,3} - C_{i3k3} \tilde{u}_{k,33} = 0, \tag{2}$$

where the Greek subscripts take a value from 1 to 2, and

$$\tilde{u}_i(y_1, y_2, x_3) = \iint u_i(x_1, x_2, x_3) \mathrm{e}^{\mathrm{i}y(a)x(a)} \, \mathrm{d}x_1 \, \mathrm{d}x_2, \tag{3}$$

in which the integral limits in both coordinates are from $-\infty$ to ∞. Solving the above ordinary differential equation yields a general solution as

$$\tilde{\boldsymbol{u}}(y_1, y_2, x_3) = \boldsymbol{a} \mathrm{e}^{-\mathrm{i}p\eta x_3}, \tag{4}$$

where η is the norm of (y_1, y_2), and p and $\boldsymbol{a}$ satisfy the eigenrelation

$$[\boldsymbol{Q} + p(\boldsymbol{R} + \boldsymbol{R}^{\mathrm{T}}) + p^2 \boldsymbol{T}]\boldsymbol{a} = 0 \tag{5}$$

with

$$Q_{ik} = C_{i\alpha k\beta} n_\alpha n_\beta, \quad R_{ik} = C_{i\alpha k3} n_\alpha, \quad T_{ik} = C_{i3k3}. \tag{6}$$

In the above, $n_1 = \cos\theta$, and $n_2 = \sin\theta$, where θ together with η are the polar coordinates of transform plane (y_1, y_2). The superscript T denotes the matrix transpose. Eshelby et al. (1953) showed that all eigenvalues of Eq. (5) cannot be real. Note that Eq. (5) is the Stroh eigenrelation for the oblique plane spanned by $(n_1, n_2, 0)$ and $(0, 0, 1)$.

Define two vectors consisting of the out-of-plane and in-plane stress components respectively as

$$t_i \equiv (\sigma_{13}, \sigma_{23}, \sigma_{33})^{\mathrm{T}} \quad \text{and} \quad s_i \equiv (\sigma_{11}, \sigma_{12}, \sigma_{22})^{\mathrm{T}}. \tag{7}$$

Applying the Fourier transforms with (x_1, x_2) and utilizing Eq. (4) through the Hooke's law $\sigma_{ij} = C_{ijkl}u_{k,l}$, we find

$$\tilde{\boldsymbol{t}} = -\mathrm{i}\eta \boldsymbol{b}\mathrm{e}^{-\mathrm{i}p\eta x_3}, \tag{8}$$

$$\tilde{\boldsymbol{s}} = -\mathrm{i}\eta \boldsymbol{c}\mathrm{e}^{-\mathrm{i}p\eta x_3}, \tag{9}$$

where

$$\boldsymbol{b} = (\boldsymbol{R}^{\mathrm{T}} + p\boldsymbol{T})\boldsymbol{a} = -\frac{1}{p}(\boldsymbol{Q} + p\boldsymbol{R})\boldsymbol{a}, \tag{10}$$

$$\boldsymbol{c} = \boldsymbol{D}\boldsymbol{a} \quad \text{with } D_{kl} = C_{1kl\alpha}n_\alpha + pC_{1kl3} \quad \text{for } k = 1,2, \text{ and } D_{3l} = C_{22l\alpha}n_\alpha + pC_{22l3}. \tag{11}$$

The six pairs of eigenvalue and associated eigenvectors, p_i, $\boldsymbol{a}_i$, $\boldsymbol{b}_i$, and $\boldsymbol{c}_i$ are arranged by

$$\mathrm{Im}\, p_i > 0, \quad p_{i+3} = \bar{p}_i, \quad \bar{\boldsymbol{a}}_{i+3} = \bar{\boldsymbol{a}}_i, \quad \boldsymbol{b}_{i+3} = \bar{\boldsymbol{b}}_i, \quad \boldsymbol{c}_{i+3} = \bar{\boldsymbol{c}}_i \qquad (i = 1,2,3),$$

$$\boldsymbol{A} = [\boldsymbol{a}_1, \boldsymbol{a}_2, \boldsymbol{a}_3], \quad \boldsymbol{B} = [\boldsymbol{b}_1, \boldsymbol{b}_2, \boldsymbol{b}_3], \quad \boldsymbol{C} = [\boldsymbol{c}_1, \boldsymbol{c}_2, \boldsymbol{c}_3],$$

where Im stands for the imaginary part and the overbar denotes the complex conjugate. Assuming that p_i are distinct, the general solutions are obtained by superposing the six solutions of Eqs. (4), (8), and (9) as

$$\tilde{\boldsymbol{u}} = \mathrm{i}\eta^{-1}\overline{\boldsymbol{A}}\langle \mathrm{e}^{-\mathrm{i}\bar{\boldsymbol{p}}\eta x_3}\rangle \boldsymbol{v} + \mathrm{i}\eta^{-1}\boldsymbol{A}\langle \mathrm{e}^{-\mathrm{i}\boldsymbol{p}\eta x_3}\rangle \boldsymbol{w}, \tag{12}$$

$$\tilde{\boldsymbol{t}} = \overline{\boldsymbol{B}}\langle \mathrm{e}^{-\mathrm{i}\bar{\boldsymbol{p}}\eta x_3}\rangle \boldsymbol{v} + \boldsymbol{B}\langle \mathrm{e}^{-\mathrm{i}\boldsymbol{p}\eta x_3}\rangle \boldsymbol{w}, \tag{13}$$

$$\tilde{\boldsymbol{s}} = \overline{\boldsymbol{C}}\langle \mathrm{e}^{-\mathrm{i}\bar{\boldsymbol{p}}\eta x_3}\rangle \boldsymbol{v} + \boldsymbol{C}\langle \mathrm{e}^{-\mathrm{i}\boldsymbol{p}\eta x_3}\rangle \boldsymbol{w}, \tag{14}$$

where $\boldsymbol{v}(\boldsymbol{y})$ and $\boldsymbol{w}(\boldsymbol{y})$ are unknown complex vectors and

$$\langle \mathrm{e}^{-\mathrm{i}\boldsymbol{p}\eta x_3}\rangle = \mathrm{diag}[\mathrm{e}^{-\mathrm{i}p_1\eta x_3}, \mathrm{e}^{-\mathrm{i}p_2\eta x_3}, \mathrm{e}^{-\mathrm{i}p_3\eta x_3}]. \tag{15}$$

It should be noted that the matrix $\boldsymbol{C}$ above is different from the fourth-order elastic stiffness tensor C_{ijkl}.

2.2. Green's function for composite laminates

Let a concentrated force $\boldsymbol{f}$ be applied at an arbitrary point (x_1^0, x_2^0, d). Applying the previous general solutions, the total solution due to the concentrated force $\boldsymbol{f}$ in the composite laminate (Fig. 1) can be written in the following form,

$$\tilde{\boldsymbol{u}}_m(y_1, y_2, x_3)\mathrm{e}^{-\mathrm{i}y_\alpha x_\alpha^0} = \tilde{\boldsymbol{u}}_m^{(s)}(y_1, y_2, x_3) + \mathrm{i}\eta^{-1}\overline{\boldsymbol{A}}_m\langle \mathrm{e}^{-\mathrm{i}\bar{\boldsymbol{p}}_m\eta(x_3 - h_{m-1})}\rangle \boldsymbol{v}_m + \mathrm{i}\eta^{-1}\boldsymbol{A}_m\langle \mathrm{e}^{-\mathrm{i}\boldsymbol{p}_m\eta(x_3 - h_m)}\rangle \boldsymbol{w}_m, \tag{16}$$

$$\tilde{\boldsymbol{t}}_m(y_1, y_2, x_3)\mathrm{e}^{-\mathrm{i}y_\alpha x_\alpha^0} = \tilde{\boldsymbol{t}}_m^{(s)}(y_1, y_2, x_3) + \overline{\boldsymbol{B}}_m\langle \mathrm{e}^{-\mathrm{i}\bar{\boldsymbol{p}}_m\eta(x_3 - h_{m-1})}\rangle \boldsymbol{v}_m + \boldsymbol{B}_m\langle \mathrm{e}^{-\mathrm{i}\boldsymbol{p}_m\eta(x_3 - h_m)}\rangle \boldsymbol{w}_m, \tag{17}$$

$$\tilde{\boldsymbol{s}}_m(y_1, y_2, x_3)\mathrm{e}^{-\mathrm{i}y_\alpha x_\alpha^0} = \tilde{\boldsymbol{s}}_m^{(s)}(y_1, y_2, x_3) + \overline{\boldsymbol{C}}_m\langle \mathrm{e}^{-\mathrm{i}\bar{\boldsymbol{p}}_m\eta(x_3 - h_{m-1})}\rangle \boldsymbol{v}_m + \boldsymbol{C}_m\langle \mathrm{e}^{-\mathrm{i}\boldsymbol{p}_m\eta(x_3 - h_m)}\rangle \boldsymbol{w}_m, \tag{18}$$

for $m = 1, 2, \ldots, n$, where the subscript m denotes the mth layer, and $\boldsymbol{v}_m$ and $\boldsymbol{w}_m$ are unknown vectors to be determined from interfacial and boundary conditions. In addition, $\tilde{\boldsymbol{u}}_m^{(s)}$, $\tilde{\boldsymbol{t}}_m^{(s)}$ and $\tilde{\boldsymbol{s}}_m^{(s)}$ are the given special solutions. According to the location of applying force $\boldsymbol{f}$, the special solutions are chosen properly such that the general-part solutions, i.e. unknown tensors $\boldsymbol{v}_m$ and $\boldsymbol{w}_m$, are nonsingular. Four cases of $\boldsymbol{f}$ applied at four different locations are considered: (1) on the top surface $(d = h_0 = 0)$; (2) in the kth layer $(h_{k-1} < d < h_k)$; (3) on the kth interface $(d = h_k)$; and (4) on the bottom surface $(h = h_n)$. These cases are described below.

In the first case where the point force is applied on the top surface $x_3 = 0$ ($d = h_0 = 0$), the special solutions are prescribed as

$$\tilde{\boldsymbol{u}}_1^{(s)} = -\mathrm{i}\eta^{-1}\overline{\boldsymbol{A}}_1\langle \mathrm{e}^{-\mathrm{i}\bar{\boldsymbol{p}}_1\eta x_3}\rangle\overline{\boldsymbol{B}}_1^{-1}\boldsymbol{f}, \tag{19}$$

$$\tilde{\boldsymbol{t}}_1^{(s)} = -\overline{\boldsymbol{B}}_1\langle \mathrm{e}^{-\mathrm{i}\bar{\boldsymbol{p}}_1\eta x_3}\rangle\overline{\boldsymbol{B}}_1^{-1}\boldsymbol{f}, \tag{20}$$

$$\tilde{\boldsymbol{s}}_1^{(s)} = -\overline{\boldsymbol{C}}_1\langle \mathrm{e}^{-\mathrm{i}\bar{\boldsymbol{p}}_1\eta x_3}\rangle\overline{\boldsymbol{B}}_1^{-1}\boldsymbol{f} \tag{21}$$

for the first layer and equal to zero for the remaining layers. Note that the above equations are the surface Green's function in a half-space derived by Willis (1966).

In the second where the point force is applied in the kth layer ($h_{k-1} < d < h_k$), the special solutions are given by

$$\tilde{\boldsymbol{u}}_k^{(s)} = \begin{cases} \mathrm{i}\eta^{-1}\boldsymbol{A}_k\langle \mathrm{e}^{-\mathrm{i}p_k\eta(x_3-d)}\rangle\boldsymbol{A}_k^{-1}\left(\boldsymbol{B}\boldsymbol{A}_k^{-1} - \overline{\boldsymbol{B}}\,\overline{\boldsymbol{A}}_k^{-1}\right)^{-1}\boldsymbol{f}, & x_3 < d, \\ \mathrm{i}\eta^{-1}\overline{\boldsymbol{A}}_k\langle \mathrm{e}^{-\mathrm{i}\bar{p}_k\eta(x_3-d)}\rangle\overline{\boldsymbol{A}}_k^{-1}\left(\boldsymbol{B}\boldsymbol{A}_k^{-1} - \overline{\boldsymbol{B}}\,\overline{\boldsymbol{A}}_k^{-1}\right)^{-1}\boldsymbol{f}, & x_3 > d, \end{cases} \tag{22}$$

$$\tilde{\boldsymbol{t}}_k^{(s)} = \begin{cases} \boldsymbol{B}_k\langle \mathrm{e}^{-\mathrm{i}p_k\eta(x_3-d)}\rangle\boldsymbol{A}_k^{-1}\left(\boldsymbol{B}\boldsymbol{A}_k^{-1} - \overline{\boldsymbol{B}}\,\overline{\boldsymbol{A}}_k^{-1}\right)^{-1}\boldsymbol{f}, & x_3 < d, \\ \overline{\boldsymbol{B}}_k\langle \mathrm{e}^{-\mathrm{i}\bar{p}_k\eta(x_3-d)}\rangle\overline{\boldsymbol{A}}_k^{-1}\left(\boldsymbol{B}\boldsymbol{A}_k^{-1} - \overline{\boldsymbol{B}}\,\overline{\boldsymbol{A}}_k^{-1}\right)^{-1}\boldsymbol{f}, & x_3 > d, \end{cases} \tag{23}$$

$$\tilde{\boldsymbol{s}}_k^{(s)} = \begin{cases} \boldsymbol{C}_k\langle \mathrm{e}^{-\mathrm{i}p_k\eta(x_3-d)}\rangle\boldsymbol{A}_k^{-1}\left(\boldsymbol{B}\boldsymbol{A}_k^{-1} - \overline{\boldsymbol{B}}\,\overline{\boldsymbol{A}}_k^{-1}\right)^{-1}\boldsymbol{f}, & x_3 < d, \\ \overline{\boldsymbol{C}}_k\langle \mathrm{e}^{-\mathrm{i}\bar{p}_k\eta(x_3-d)}\rangle\overline{\boldsymbol{A}}_k^{-1}\left(\boldsymbol{B}\boldsymbol{A}_k^{-1} - \overline{\boldsymbol{B}}\,\overline{\boldsymbol{A}}_k^{-1}\right)^{-1}\boldsymbol{f}, & x_3 > d \end{cases} \tag{24}$$

for the kth layer in which $\boldsymbol{f}$ is applied, and equal to zero for all of the other layers. The above special solutions are the infinite-space Green's function, whose physical counterparts can be evaluated analytically by Ting and Lee (1997) and Pan and Yuan (2000a,b).

In the third case where the point force is applied on the interface $x_3 = h_{k-1}$ between the $(k-1)$th and kth layer ($d = h_{k-1}$), the special solutions are assigned to be the interfacial Green's functions of bimaterials (Ting, 1996),

$$\tilde{\boldsymbol{u}}_{k-1}^{(s)} = \mathrm{i}\eta^{-1}\boldsymbol{A}_{k-1}\langle \mathrm{e}^{-\mathrm{i}\boldsymbol{p}_{k-1}\eta(x_3-h_{k-1})}\rangle\boldsymbol{A}_{k-1}^{-1}\left(\boldsymbol{B}_{k-1}\boldsymbol{A}_{k-1}^{-1} - \overline{\boldsymbol{B}}_k\overline{\boldsymbol{A}}_k^{-1}\right)^{-1}\boldsymbol{f}, \tag{25}$$

$$\tilde{\boldsymbol{t}}_{k-1}^{(s)} = \boldsymbol{B}_{k-1}\langle \mathrm{e}^{-\mathrm{i}\boldsymbol{p}_{k-1}\eta(x_3-h_{k-1})}\rangle\boldsymbol{A}_{k-1}^{-1}\left(\boldsymbol{B}_{k-1}\boldsymbol{A}_{k-1}^{-1} - \overline{\boldsymbol{B}}_k\overline{\boldsymbol{A}}_k^{-1}\right)^{-1}\boldsymbol{f}, \tag{26}$$

$$\tilde{\boldsymbol{s}}_{k-1}^{(s)} = \boldsymbol{C}_{k-1}\langle \mathrm{e}^{-\mathrm{i}\boldsymbol{p}_{k-1}\eta(x_3-h_{k-1})}\rangle\boldsymbol{A}_{k-1}^{-1}\left(\boldsymbol{B}_{k-1}\boldsymbol{A}_{k-1}^{-1} - \overline{\boldsymbol{B}}_k\overline{\boldsymbol{A}}_k^{-1}\right)^{-1}\boldsymbol{f}, \tag{27}$$

$$\tilde{\boldsymbol{u}}_k^{(s)} = \mathrm{i}\eta^{-1}\overline{\boldsymbol{A}}_k\langle \mathrm{e}^{-\mathrm{i}\bar{\boldsymbol{p}}_k\eta(x_3-h_{k-1})}\rangle\overline{\boldsymbol{A}}_k^{-1}\left(\boldsymbol{B}_{k-1}\boldsymbol{A}_{k-1}^{-1} - \overline{\boldsymbol{B}}_k\overline{\boldsymbol{A}}_k^{-1}\right)^{-1}\boldsymbol{f}, \tag{28}$$

$$\tilde{\boldsymbol{t}}_k^{(s)} = \overline{\boldsymbol{B}}_k\langle \mathrm{e}^{-\mathrm{i}\bar{\boldsymbol{p}}_k\eta(x_3-h_{k-1})}\rangle\overline{\boldsymbol{A}}_k^{-1}\left(\boldsymbol{B}_{k-1}\boldsymbol{A}_{k-1}^{-1} - \overline{\boldsymbol{B}}_k\overline{\boldsymbol{A}}_k^{-1}\right)^{-1}\boldsymbol{f}, \tag{29}$$

$$\tilde{\boldsymbol{s}}_k^{(s)} = \overline{\boldsymbol{C}}_k\langle \mathrm{e}^{-\mathrm{i}\bar{\boldsymbol{p}}_k\eta(x_3-h_{k-1})}\rangle\overline{\boldsymbol{A}}_k^{-1}\left(\boldsymbol{B}_{k-1}\boldsymbol{A}_{k-1}^{-1} - \overline{\boldsymbol{B}}_k\overline{\boldsymbol{A}}_k^{-1}\right)^{-1}\boldsymbol{f} \tag{30}$$

for the $(k-1)$th and kth layers that share the interface. In all of the other layers, the special solutions are equal to zero.

In the last case where the point force is applied at the bottom surface ($x_3 = d = h_n$), which is similar to the first case, the surface Green's function of an upper half-space is used to substitute the special solution of the nth layer. Otherwise, the special solution is taken to be equal to zero. This is written as

$$\tilde{\boldsymbol{u}}_n^{(s)} = \mathrm{i}\eta^{-1}\boldsymbol{A}_n\langle \mathrm{e}^{-\mathrm{i}\boldsymbol{p}_n\eta(x_3-h_n)}\rangle \boldsymbol{B}_n^{-1}\boldsymbol{f}, \tag{31}$$

$$\tilde{\boldsymbol{t}}_n^{(s)} = \boldsymbol{B}_n\langle \mathrm{e}^{-\mathrm{i}\boldsymbol{p}_n\eta(x_3-h_n)}\rangle \boldsymbol{B}_n^{-1}\boldsymbol{f}, \tag{32}$$

$$\tilde{\boldsymbol{s}}_n^{(s)} = \boldsymbol{C}_n\langle \mathrm{e}^{-\mathrm{i}\boldsymbol{p}_n\eta(x_3-h_n)}\rangle \boldsymbol{B}_n^{-1}\boldsymbol{f}. \tag{33}$$

To obtain the unknown general-part solution, we consider a proportional spring-type boundary condition for the top and bottom surfaces, expressed as

$$\boldsymbol{G}_1\boldsymbol{u}_1 + \boldsymbol{H}_1\boldsymbol{t}_1 = 0 \quad \text{at } x_3 = 0, \qquad \boldsymbol{G}_n\boldsymbol{u}_n + \boldsymbol{H}_n\boldsymbol{t}_n = 0 \quad \text{at } x_3 = h_n, \tag{34}$$

where $\boldsymbol{G}_1$, $\boldsymbol{H}_1$, $\boldsymbol{G}_n$, and $\boldsymbol{H}_n$ are given constant matrices. The continuity in displacement and traction along the interfaces requires

$$\boldsymbol{u}_{m-1} = \boldsymbol{u}_m, \quad \boldsymbol{t}_{m-1} = \boldsymbol{t}_m \qquad \text{at } x_3 = h_m. \tag{35}$$

Substituting Eqs. (16) and (17) into Eqs. (34) and (35) yields following linear system of algebraic equations:

$$\boldsymbol{E}\boldsymbol{q} = \boldsymbol{\beta}, \tag{36}$$

where $q(\equiv [\boldsymbol{v}_1^{\mathrm{T}}, \boldsymbol{w}_1^{\mathrm{T}}, \ldots, \boldsymbol{v}_m^{\mathrm{T}}, \boldsymbol{w}_m^{\mathrm{T}}, \ldots, \boldsymbol{v}_n^{\mathrm{T}}, \boldsymbol{w}_n^{\mathrm{T}}]_{6n}^{\mathrm{T}})$ is an unknown vector, $\boldsymbol{\beta}$ is a constant vector of the same dimension as $\boldsymbol{q}$, and $\boldsymbol{E}$ is the stiffness matrix of dimensions $6n \times 6n$. If $\boldsymbol{E}$ is invertible, the unknown vectors $\boldsymbol{v}_m$ and $\boldsymbol{w}_m$ can be solved for all layers at a given point $\boldsymbol{y}$ in the Fourier transformed domain. By substituting them back into Eqs. (16)–(18), the Green's displacement and stress are obtained in the transformed domain.

Once the transformed-domain solutions are derived, the physical-domain Green's function due to a point force is derived by using Fourier inverse transform as

$$u_i(x_1, x_2, x_3) = \frac{1}{(2\pi)^2}\iint \tilde{u}_i(y_1, y_2, x_3)\mathrm{e}^{-\mathrm{i}y_\alpha x_\alpha}\,\mathrm{d}y_1\,\mathrm{d}y_2, \tag{37}$$

where the integral limits in both coordinates are from $-\infty$ to ∞. Or, the inverse transform may be carried out, sometimes more conveniently, in the polar coordinates,

$$u_i(x_1, x_2, x_3) = \frac{1}{(2\pi)^2}\iint \eta\tilde{u}_i(y_1, y_2, x_3)\mathrm{e}^{-\mathrm{i}y_\alpha x_\alpha}\,\mathrm{d}\eta\,\mathrm{d}\theta, \tag{38}$$

where the integral limit in η is from 0 to ∞, and in θ from 0 to 2π.

3. Numerical examples

For an infinite composite laminate with finite thickness, not all kinds of boundary conditions lead to meaningful physical solutions due to a point force. In some cases, a physical solution does not even exist. For example, for an infinite plate, to impose traction-free boundary condition along both the top and bottom surfaces results in an indefinite displacement (not just singular) due to any type of out-of-plane loading, concentrated or distributed. In these cases, the corresponding Fourier transformed domain solutions are not meaningful.

In the following, we apply the previous formulation to examine the three-dimensional displacement and stress in composite laminates due to a point force under a couple of common types of boundary conditions. A composite laminate of ten plies of identical orthogonal materials with stacking sequence $(0/30/-30/90/45/-45/0/60/-60/90)$ is considered. The orthotropic material represents a unidirectional fiber-reinforced composite plate, with the fibers lying in the horizontal plane. The number in the stacking sequence indicates the in-plane rotation angle of each ply relative to the reference 0°-ply where the fibers lie in the 0° direction. The elastic constants are given by $E_1 = 138$ GPa, $E_2 = E_3 = 14.5$ GPa, $\mu_{23} = \mu_{13} = \mu_{12} = 5.86$ GPa, and $v_{23} = v_{13} = v_{12} = 0.21$. E_1 will be used to normalize the stress quantities. The total thickness of the laminate is H, and hence that of each ply is $0.1H$. H will be used to normalize quantities of length dimension, such as coordinate and displacement. A computational efficient numerical technique (Yang and Pan, 2002) is used to carry out the numerical integral of the Green's functions.

3.1. Case 1: One surface being displacement-fixed

First considered is the case of the laminate with one surface being displacement-fixed and the other one free of traction. This is expressed, corresponding to Eq. (34) as

$$\boldsymbol{G}_1 = 0, \quad \boldsymbol{H}_1 = \boldsymbol{I}_{3\times3}, \quad \boldsymbol{G}_n = \boldsymbol{I}_{3\times3}, \quad \boldsymbol{H}_n = 0, \tag{39}$$

where $\boldsymbol{I}$ is the identity matrix. Also supposed is a unit point force applied at $(0,0,0)$ on the traction-free surface in either one of the three coordinates (Fig. 1). The displacement and stress induced by the point force are evaluated at points along a circle around the loading point on the traction-free surface, and along a vertical line from $(H,0,0)$ to $(H,0,H)$. In the former case, the radius of the circle is H. The results are plotted in Figs. 2–5.

Figs. 2 and 3 show the variation of displacement and nonzero (in-plane) stress components along the circle due to the point force applied in the x_3-axis and in the x_2-axis respectively. It can be seen that both of the displacement and stress are at significant variance along the circle due to the complicated layup of the composite laminate. Figs. 4 and 5 show the variation of displacement and nonzero (in-plane) stress components along the vertical line due to the point force applied along the x_3-axis and along the x_2-axis respectively. These results show that the boundary conditions on the laminate surfaces and the interfacial continuity conditions between the different plies are satisfied, suggesting the validity of the previous formulation. The in-plane stress components are discontinuous across the interfaces, as expected due to the discontinuity of materials properties. On the other hand, their vertical variations in the individual plies are

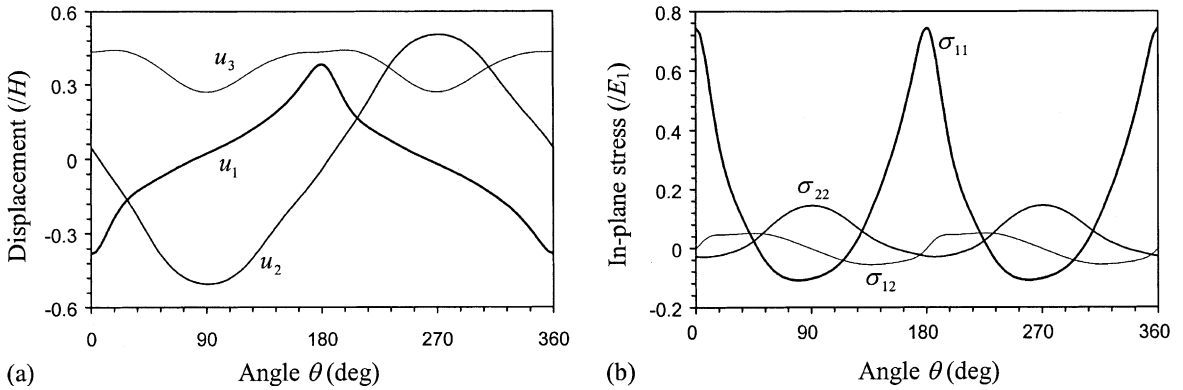

Fig. 2. Variation of normalized displacement and nonzero stress components along a circle $(H\cos\theta, H\sin\theta, 0)$ due to a surface unit point force applied in the x_3-axis (Case 1).

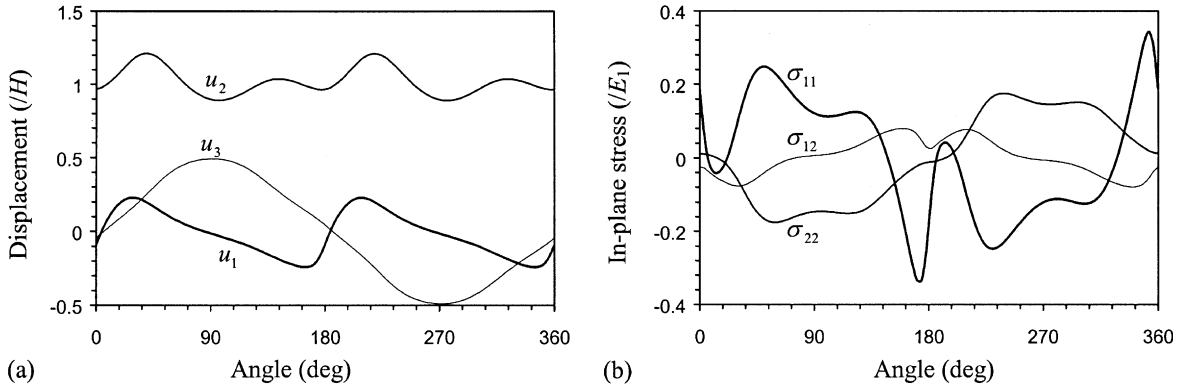

Fig. 3. Variation of normalized displacement and stress components along a vertical line $(H, 0, x_3)$ due to a surface unit point force applied in the x_3-axis (Case 1).

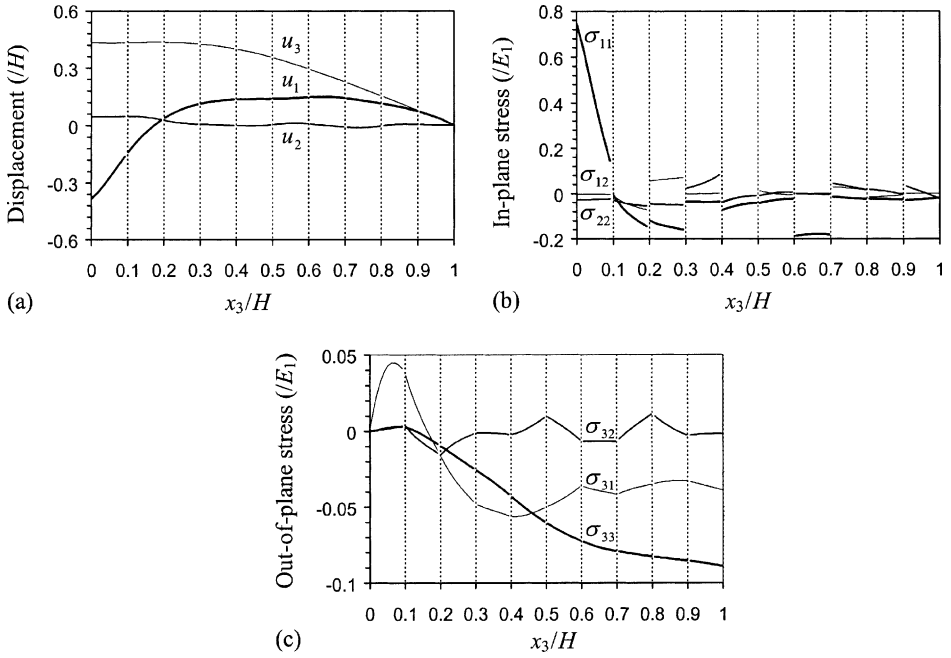

Fig. 4. Variation of normalized displacement and nonzero stress components along a circle $(H\cos\theta, H\sin\theta, 0)$ due to a surface unit point force applied in the x_2-axis (Case 1).

intriguing that in some plies, the stress components, for example, σ_{11}, increase with distance to the loading point, but decrease in the others. The continuous out-of-plane stress components show kinks across the interfaces between different plies, i.e., lack of continuity in their vertical-direction derivatives.

3.2. Case 2: One surface being mirror-symmetric

Let us consider the case of the laminate with one surface being mirror-symmetric and the other one free of traction. This is expressed, corresponding to Eq. (34) as

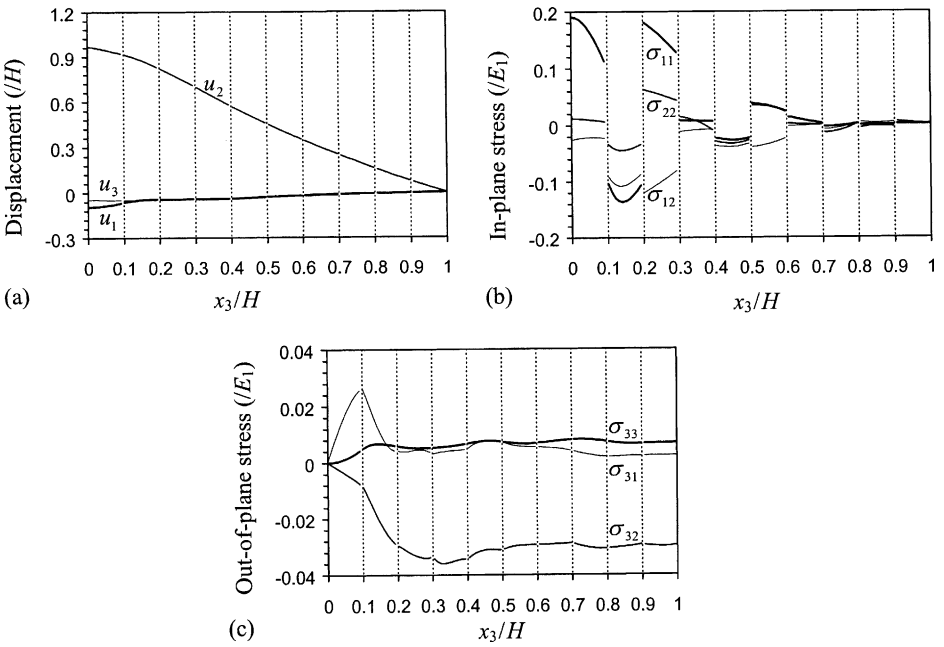

Fig. 5. Variation of normalized displacement and stress components along a vertical line $(H, 0, x_3)$ due to a surface unit point force applied in the x_2-axis (Case 1).

$$\boldsymbol{G}_1 = 0, \quad \boldsymbol{H}_1 = \boldsymbol{I}_{3\times 3}, \quad \boldsymbol{G}_n = \begin{pmatrix} 0 & 0 & 0 \\ 0 & 0 & 0 \\ 0 & 0 & 1 \end{pmatrix}, \quad \boldsymbol{H}_n = \begin{pmatrix} 1 & 0 & 0 \\ 0 & 1 & 0 \\ 0 & 0 & 0 \end{pmatrix}. \tag{40}$$

The same as in Case 1, a unit point force is applied at $(0, 0, 0)$ on the traction-free surface. The displacement and stress induced by the point force are evaluated at points along a circle of radius H around the loading point on the traction-free surface, and along a vertical line from $(H, 0, 0)$ to $(H, 0, H)$. The results are plotted in Figs. 6–9.

Similar to the previous Figs. 2–5, Figs. 6 and 7 show the variation of displacement and nonzero (in-plane) stress components along the circle due to the point force applied in the x_3-axis and x_2-axis respectively.

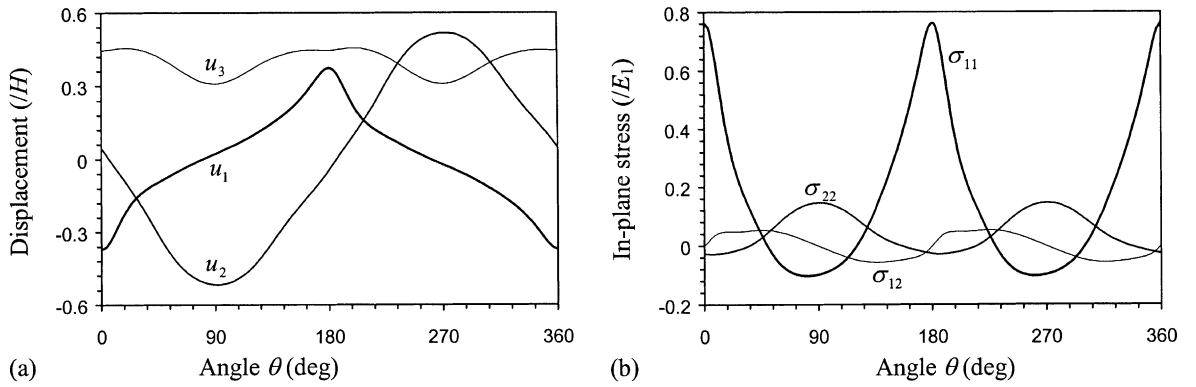

Fig. 6. Variation of normalized displacement and nonzero stress components along a circle $(H\cos\theta, H\sin\theta, 0)$ due to a surface unit point force applied in the x_3-axis (Case 2).

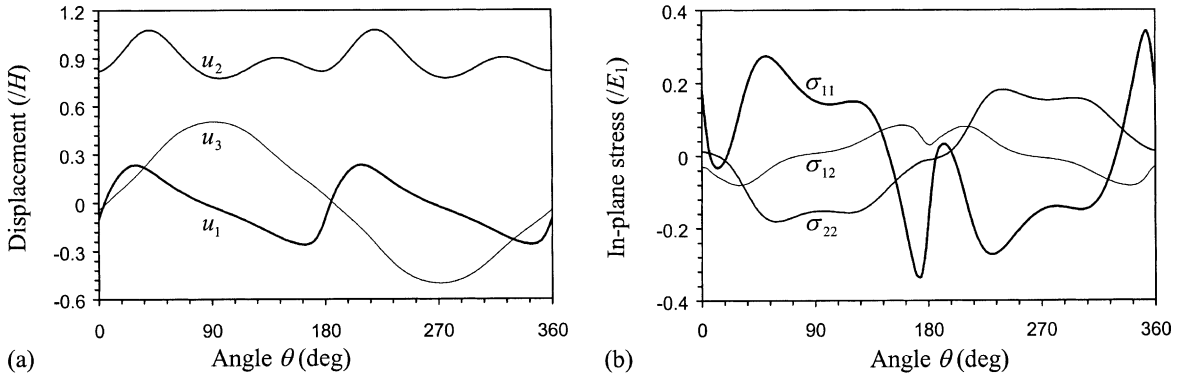

Fig. 7. Variation of normalized displacement and stress components along a vertical line $(H, 0, x_3)$ due to a surface unit point force applied in the x_3-axis (Case 2).

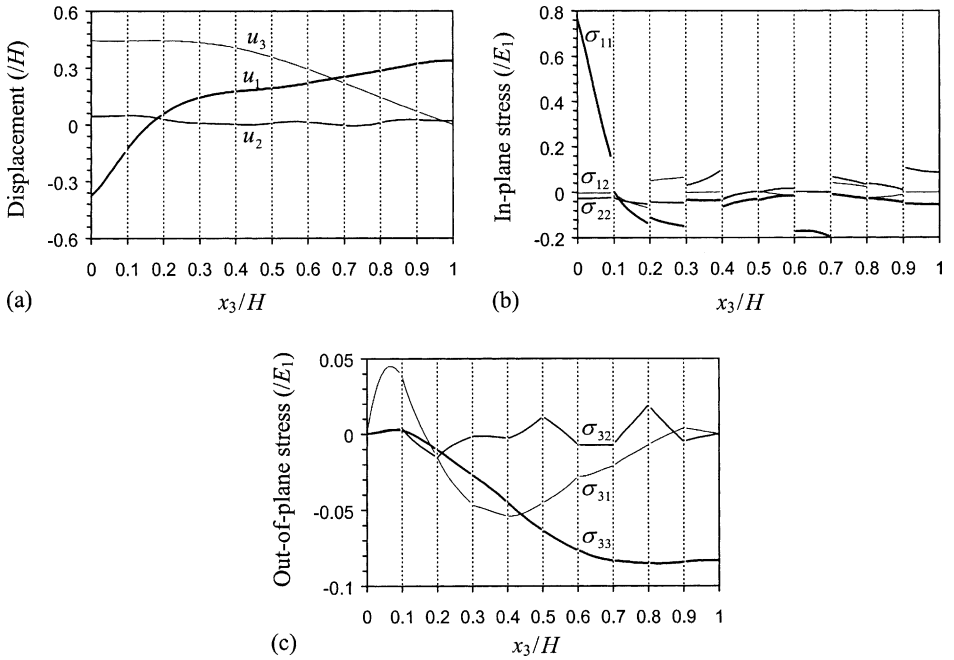

Fig. 8. Variation of normalized displacement and nonzero stress components along a circle $(H\cos\theta, H\sin\theta, 0)$ due to a surface unit point force applied in the x_2-axis (Case 2).

Figs. 8 and 9 show the variation of displacement and nonzero (in-plane) stress components along the vertical line due to the point force applied along the x_3-axis and x_2-axis respectively. As compared to the previous case, these results show very similar characteristics, such as the satisfaction of boundary and interfacial conditions. Also, it is seen that the change of the boundary condition (on the opposite surface to where the point force is applied) makes a little change on the displacement and stress fields, especially the stress field, along the circle on the traction-free surface. On the other hand, these fields are altered significantly as the observation point gets closer to the surface where the boundary conditions are altered.

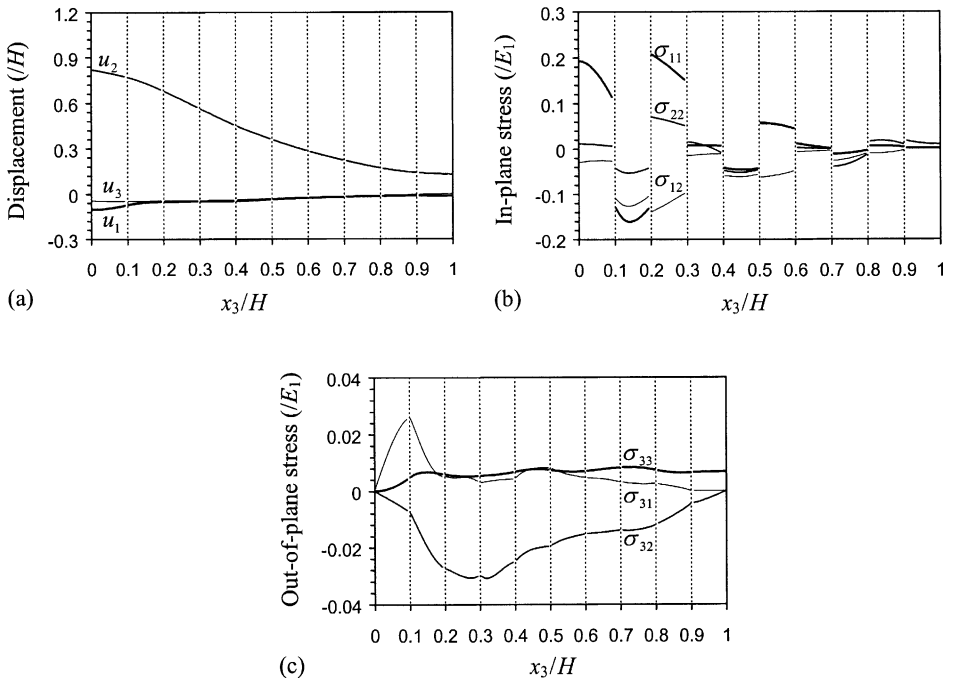

Fig. 9. Variation of normalized displacement and stress components along a vertical line $(H, 0, x_3)$ due to a surface unit point force applied in the x_2-axis (Case 2).

4. Conclusions

Three-dimensional Green's functions due to a point force in generally anisotropic composite laminates have been derived within the framework of extended Stroh formalism and Fourier transforms. The interfaces between different plies are perfectly bonded. The Green's functions for the point forces applied at the free surface, interface, and in the interior of a layer have been derived in the Fourier transformed domain respectively. A proportional spring-type boundary condition is imposed on the top and bottom surfaces. The spring-type boundary condition may be reduced to traction-free, displacement-fixed, and mirror-symmetric conditions. Since the Green's functions are attained in the Fourier transformed domain, Fourier inverse transform is performed using a computational efficient numerical approach to express the Green's functions in the physical domain so that they can be implemented in the boundary element method.

Numerical examples have been given with a ten-layered orthotropic composite laminate with one surface being displacement-fixed or mirror-symmetric and the other one being free of traction. The results showed that the boundary and interfacial continuity conditions are satisfied in the computed Green's solutions, suggesting the validity of the present formulation and computational algorithm. The interesting characteristics of the Green's fields due to a surface point force have also been discussed. These fields are rather complicated in the composite laminate.

Because the Green's functions satisfy the interlaminar continuities and top and bottom traction-free surfaces, modeling of the problems such as composite laminates with cutouts using boundary element method becomes truly two-dimensional and discretization is only needed along the cutouts and lateral outer boundaries. Therefore, in designing the composite bolted joints with many layers, the boundary element method is robust and offers much better solution accuracy in modeling joints of complex geometries (Pan et al., 2001; Yang et al., submitted for publication).

Acknowledgement

This research is supported by the Air Force Office of Scientific Research under grant no. F49620-95-1-0256.

References

Barnett, D.M., Lothe, J., 1973. Synthesis of the sextic and the integral formalism for dislocations, Green functions, and surface waves in anisotropic elastic solids. Physica Norvegica 7, 13–19.

Barnett, D.M., Lothe, J., 1975. Line force loadings on anisotropic half-spaces and wedges. Physica Norvegica 8, 13–22.

Boussinesq, J., 1885. Application des potentials à l' etude de l' équilibre et du Mouvement des Solids Elastiques. Gauthier-Villars, Paris.

Cerruti, V., 1888. Atti della academia dei nazinale lincei, classe di scienze fisiche mathematiche e naturati. Roma, Acc. Linc. Rend., Series 4.

Elliott, H.A., 1948. Three-dimensional stress distributions in hexagonal aeolotropic crystals. Proceedings, Cambridge Philosophical Society 44, 522–533.

Eshelby, J.D., Reed, W.T., Shockley, W., 1953. Anisotropic elasticity with applications to dislocation theory. Acta Metallurgica 1, 251–259.

Fredholm, I., 1900. Sur les equations de léquilibre d'un corps solide elastique. Act Math. 23, 1–42.

Green, A.E., Zerna, W., 1954. Theoretical Elasticity. The Clarendon Press, Oxford (Chapter 6).

Kroner, E., 1953. Das fundamentalintegral der anisotropen elastischen differentialgeichungen. Zeitschrift fur Physics 136, 402–410.

Lejcek, L., 1965. The Green function of the theory of elasticity in an anisotropic media. Quarterly Journal of Mechanics and Applied Mathematics 18, 419–433.

Lekhnitskii, S.G., 1963. Theory of Elasticity of an Anisotropic Elastic Body. Holden-Day, San Francisco.

Lifshitz, I.M., Rozenzweig, L.N., 1947. On the construction of the Green's tensor for the basic equation of the theory of elasticity of an anisotropic infinite medium. Zhurnal Eksperimentalnoi i Teoreticheskoi Fiziki 17, 783–791.

Mindlin, D., 1936. Force at a point in the interior of a semi-infinite solid. Physics 7, 195–202.

Mura, T., 1987. Micromechanics of Defects in Solids, second ed. Martinus Nijhoff Publishers, Dordrecht, The Netherlands.

Pan, Y.C., Chou, T.W., 1976. Point force solution for an infinite transversely isotropic solid. ASME Journal of Applied Mechanics 43, 608–612.

Pan, Y.C., Chou, T.W., 1979a. Green's functions for two-phase transversely isotropic materials. International Journal of Engineering Sciences 17, 545–551.

Pan, Y.C., Chou, T.W., 1979b. Green's functions for two-phase transversely isotropic materials. ASME Journal of Applied Mechanics 46, 551–556.

Pan, E., 1997. Static Green's functions in multilayered half spaces. Applied Mathematical Modeling 21, 509–521.

Pan, E., Yuan, F.G., 2000a. Three-dimensional Green's functions in anisotropic bi-materials. International Journal of Solids and Structures 37, 5329–5351.

Pan, E., Yuan, F.G., 2000b. Three-dimensional Green's functions in anisotropic piezoelectric bi-materials. International Journal of Engineering Science 38, 1939–1960.

Pan, E., Yang, B., Cai, G., Yuan, F.G., 2001. Stress analysis around holes in composite laminates using boundary element method. Engineering Analysis with Boundary Element 25, 31–40.

Stroh, A.N., 1958. Dislocations and cracks in anisotropic elasticity. Philosophical Magazine 3, 625–646.

Stroh, A.N., 1962. Steady state problems in anisotropic elasticity. Journal of Mathematical Physics 41, 77–103.

Synge, J.L., 1957. The Hypercircle in Mathematical Physics. Cambridge University Press.

Thomson, M. (Lord Kelvin), 1848. Note on the integration of the equations of equilibrium of an elastic solid. Cambridge and Dublin Mathematical Journal, 76–99.

Ting, T.C.T., 1996. Anisotropic Elasticity. Oxford University Press, Oxford.

Ting, T.C.T., Lee, V., 1997. The three-dimensional elastostatic Green's function for generally anisotropic elastic solids. Quarterly Journal of Mechanics and Applied Mathematics 50, 407–426.

Wang, C.Y., 1997. Elastic fields produced by a point source in solids of general anisotropy. Journal of Engineering Mathematics 32, 41–52.

Willis, J.R., 1966. Hertzian contact of anisotropic bodies. Journal of the Mechanics and Physics of Solids 14, 163–176.

Willis, J.R., 1969. The Green function of the theory of elasticity in an anisotropic hexagonal medium. Cezch Journal of Physics, Series B 19, 799–803.

Yang, B., Pan, E., 2002. Efficient evaluation of three-dimensional Green's functions in anisotropic elastoelastic multilayered composites. Engineering Analysis with Boundary Element 26, 355–366.

Yang, B., Pan, E., Yuan, F.G., submitted for publication. Three-dimensional stress analyses in composite laminates with an elastically pinned hole. International Journal of Solids and Structures.

Yue, Z.Q., 1999. Layered elastic model for analysis of cone penetration testing. International Journal for Numerical and Analytical Methods in Geomechanics 23, 829–843.